NASA TM-88584

HOVER AND FORWARD FLIGHT ACOUSTICS AND PERFORMANCE OF A SMALL-SCALE HELICOPTER ROTOR SYSTEM

Cahit Kitaplioglu
NASA Ames Research Center
Moffett Field, California 94035, U.S.A.

and

Patrick Shinoda
Aeroflightdynamics Directorate
U.S. Army Aviation Research and Technology Activity--AVSCOM
NASA Ames Research Center
Moffett Field, California 94035, U.S.A.

September 10-13, 1985

London, England

THE CITY UNIVERSITY, LONDON, EC1V OHB, ENGLAND

HOVER AND FORWARD FLIGHT ACOUSTICS AND PERFORMANCE OF A SMALL-SCALE HELICOPTER ROTOR SYSTEM

Cahit Kitaplioglu* and Patrick Shinodat
NASA Ames Research Center, Moffett Field, California 94035

ABSTRACT

A 2.1-m diam., 1/6-scale model helicopter main rotor was tested in hover in the test section of the NASA Ames 40- by 80-Foot Wind Tunnel. Subsequently, it was tested in forward flight in the Ames 7- by 10-Foot Wind Tunnel. The primary objective of the tests was to obtain performance and noise data on a small-scale rotor at various thrust coefficients, tip Mach numbers, and, in the latter case, various advance ratios, for comparison with similar existing data on full-scale helicopter rotors. This comparison yielded a preliminary evaluation of the scaling of helicopter rotor performance and acoustic radiation in hover and in forward flight. Correlation between model-scale and full-scale performance and acoustics was quite good in hover. In forward flight, however, there were significant differences in both performance and acoustic characteristics. A secondary objective was to contribute to a data base that will permit the estimation of facility effects on acoustic testing.

1. INTRODUCTION

Because of the wide availability of small wind tunnels, there are advantages in using model-scale instead of full-scale rotors for exploratory research. However, there is a lower limit to the model size that will yield accurate aerodynamic and acoustic information. This restriction arises from limitations in aerodynamic and dynamic scaling, fabrication, and hardware and instrumentation size requirements. In addition, geometrical scaling may require that proportionately higher acoustic frequencies be dealt with, although it is not presently known whether all sources of rotor noise scale geometrically. Therefore, microphone and tape-recorder frequency response limitations also restrict the smallest practical scale. Rotor systems that are about 1/5 to 1/7 scale are widely used in aerodynamic, dynamic, and acoustic testing. In general, these scale models are compatible with existing test facilities.

Several studies of the scaling of helicopter rotors have been reported. Schmitz and his co-workers (Refs. 1-3) made extensive scaling studies of both high-speed and blade-vortex interaction noise on

*Aerospace Engineer, Rotary-Wing Aeromechanics Branch, NASA.
†Aerospace Engineer, Aeroflightdynamics Directorate, U.S. Army Aviation Research and Technology Activity--AVSCOM.

two-bladed rotors. Their main focus was on impulsive noise arising from both compressibility and blade-vortex interaction effects. They have concentrated on the detectability problem, which is essentially a function of the low-frequency harmonic, rather than broadband, components of the radiated acoustic energy.

The work of Leighton et al. (Ref. 4) deals with very small scale models. As pointed out earlier, aside from scaling questions, there are practical disadvantages to testing at such small scale. In any case, Leighton's conclusions indicate that 1/20 scale is too small to yield consistent data, except for relative trends at high tip Mach numbers. So there is room for further work in the area of rotor-noise scaling. Because data from several tests are required if clear-cut trends are to be perceived, it may be some time before satisfactory scaling rules for all rotor-noise mechanisms become available.

The work reported in this paper centers on four-bladed rotors with state-of-the-art airfoils. During a series of hover tests conducted in the NASA Ames 40- by 80-Foot Wind Tunnel test section, and of forward-flight tests conducted in the 7- by 10-Foot Wind Tunnel, performance and acoustic data were obtained on a 2.1-m diam, 1/6-scale model of a helicopter main rotor.

By comparing data obtained during this series of tests with existing full-scale hover and forward-flight data, a preliminary attempt was made to evaluate the extent to which model-scale experiments can reproduce full-scale effects.

The facilities of the National Full Scale Aerodynamic Complex (NFAC) provide the capability of testing both full-scale and model-scale rotors in the same wind tunnel. Eventually an extensive, consistent data base will permit a definitive evaluation of scale effects. Future tests in this series will include a hover experiment at the Ames Outdoor Aerodynamic Research Facility and forward-flight tests in the 40- by 80-Foot/80- by 120-Foot Wind Tunnel. Additional full-scale tests in the latter will supplement existing full-scale data.

The full-scale data used in this study are (1) those obtained during a 1977 test in the 40- by 80-Foot Wind Tunnel (Refs. 5 and 6);(2) those obtained during a hover stand test of a Sikorsky S-76 rotor system (Ref. 7); and (3) those obtained during an S-76 hover and flight test by the Federal Aviation Administration (Ref. 8).

2. DESCRIPTION OF TEST HARDWARE

The 2.1-m diam four-bladed rotor was mounted on the fully articulated rotor-head of the Ames Rotor Test Rig (RTR) (Fig. 1). The carbon/fiberglass composite blades are dynamically and geometrically representative of the Sikorsky S-76 rotor blades (Table 1) except that the model blades have rectangular tips. The rotor-head allows collective and cyclic pitch control. Lead-lag, coning, and cyclic flapping are

measured by variable potentiometers. The entire test-rig assembly can be tilted, either pitched up or down.

The RTR incorporates a six-component strain-gauge internal balance to measure steady-state rotor forces and moments. In addition, the rotor torque is measured by a load cell. Several sets of blade strain gauges and a number of accelerometers on both the metric and nonmetric portions of the RTR are used to monitor loads and vibration levels for safety purposes during testing. All the performance and safety data were appropriately filtered, digitized, and recorded on the data-acquisition-system computer. Both steady-state and time-varying information were available. Important test parameters such as rotor rotational tip Mach number, C_L/σ, and shaft angle were displayed in real time. This permitted test conditions for the different runs to be accurately established.

3. HOVER TEST

Test Description

The hover test was performed in the NASA Ames 40- by 80-Foot Wind Tunnel test section. The rotor assembly was mounted in a thrust-down/wake-up mode, with the hub 3 m above the floor (Fig. 2). This configuration avoided ground-effect influences and allowed the test stand to be located on the low-velocity inflow side of the rotor disk. The wake had a large unobstructed space to which to exhaust.

The 40- by 80-Foot Wind Tunnel test section has a 15-cm-thick acoustic lining installed on the floor, ceiling, and walls. It consists of open-cell foam covered with perforated steel decking, and has an absorption coefficient greater than 0.9 above 1 kHz, which decreases approximately linearly to 0.5 at 100 Hz.

The lining performed well in absorbing wall reflections, as determined by a series of impulsive source measurements made before testing began. This consisted of firing a starter pistol and recording the impulsive transient waveform. The pistol was fired from several locations corresponding to different source locations. For most microphones and source positions only a single pulse corresponding to the incident wave was observed; there were no significant secondary pulses. For a few of the microphones, a secondary pulse having a relatively high amplitude was also observed. From the measured delay times, the probable reflection points were identified to be localized flat areas such as the bases of some of the microphone stands and the RTR mount. After covering those areas with 7.5-cm-thick foam, these reflections were eliminated. The final test setup was judged to be acoustically quite good.

An array of five microphones was mounted in a single vertical plane at distances of 1, 1.5, and 2 rotor diameters and at angles of 10°, 30°, and 45° "below" the rotor plane (Fig. 3), which actually

correspond to positions above the rotor plane for the thrust-down mode. Microphone No. 4 was placed as an image of No. 5 "above" the rotor plane. Two microphones were placed 30° to either side of the main array.

The microphone placement scheme was chosen to include the estimated directional locations appropriate for major hover noise generation mechanisms. Thickness noise is radiated mostly near the rotor plane. The two image microphones above and below the rotor plane allow an evaluation of asymmetric radiation patterns. The microphones at larger angles were placed to measure rotational loading noise caused by thrust and torque. Turbulence ingestion noise, which is important in hover, is expected to have a broad directivity "below" the rotor and should be adequately captured by the 45° microphone. The latter is also well placed for detecting blade-vortex interaction noise, when present.

Acoustic signals were measured with 1.27-cm, free-field response-type microphones, mounted such that their axes were parallel with the tunnel axis and facing the rotor. Since the exact locations of the noise sources were not known, this provided a standardized scheme for comparison with other experiments. Standard protective grids were placed over the microphone cartridges. Wind screens were not used because no appreciable wake flow was estimated to be present at the microphone positions.

Microphone outputs were recorded on a 14-track, FM instrumentation tape recorder, set up to IRIG Wideband I standards at 30 in./sec (76.2 cm/sec). The system frequency response was good to approximately 20 kHz. 1/rev, 1024/rev, and time-code signals were also recorded. Test conditions and amplifier information were annotated on the edge track.

During test set up, an extensive set of measurements was made to check the frequency response of each channel; a wide-band, white-noise signal was electronically injected into each cathode follower. During testing, a piston-phone calibration was performed on each microphone before the start of each day's runs.

Hover Performance Results

The primary variables during the hover test were tip Mach number and rotor thrust coefficient:

Rotor-tip Mach number, M_{tip}	0.55, 0.627
Rotor thrust coefficient, C_T/σ	0 - 0.12

Figures 4 and 5 summarize the model-rotor hover performance data obtained during the hover test. Also included in these figures are two additional sets of hover performance data obtained on a full-scale Sikorsky S-76 rotor. One set was obtained during a test in the 40- by

80-Foot Wind Tunnel (Ref. 5); the second set was obtained during a hover-stand test at Sikorsky Aircraft (Ref. 7). Note that the tip Mach number of the model-scale test is somewhat different from that of the full-scale tests. Also, both full-scale tests utilized a swept tapered tip profile rather than a rectangular tip. The full-scale whirl-stand data have been reduced by 3% to account for test-stand interference and ground effects. The small differences in tip Mach number and tip shape are not believed to be significant in hover, especially in view of the corrections made to the whirl-tower data. It should also be noted that the full-scale hover data obtained in the 40- by 80-Foot Wind Tunnel is for -10° shaft angle, rather than 0°, and with tunnel walls open to reduce recirculation effects (Ref. 7).

The model-scale and full-scale data compare very well. At high thrusts ($C_T/\sigma > 0.10$) where the small-scale rotor would be expected to stall earlier, no full-scale data were obtained.

Figure 5 shows that the model-scale rotor required greater power input than the full-scale rotor to achieve a given thrust level. The difference in power requirements is quite significant (approximately 25%) at low thrust, but diminishes to about 4%-5% at maximum thrust. The higher power required at low thrust is consistent with expected influence of Reynolds number on profile power.

Hover Acoustic Results

Space limitations preclude a detailed discussion of the acoustic data with respect to variations in directivity angle, distance, and operating conditions. This section concentrates on the specific topic of acoustic scaling effects. Acoustic data obtained during this test were compared with data obtained by the FAA during a flight test of a Sikorsky S-76 helicopter which included some hover runs (Ref. 8). Duplicate tapes of the FAA hover-noise test results were provided to NASA, and data reduction was performed at Ames.

Table 2 compares the important parameters of the two tests. Some differences do exist, but they should not significantly affect the conclusions. More importantly, the FAA data were obtained with the aircraft operating in ground effect. Therefore, the comparisons and conclusions of this section must be regarded as preliminary.

The most striking feature typical of the data obtained during the model-scale hover test is its variability in time (statistical nonstationarity) at fixed operating conditions. Figures 6a and 6b are two waveforms observed at slightly different times during the same run point. This variability is thought to be related to recirculation patterns existing in the confined environment of the test section even though its dimensions were very large in comparison to model size.

Subjectively, the noise corresponding to the impulsive waveform (Fig. 6a) was judged to be loud and had the "popping" quality typical of blade slap. On the other hand, the noise associated with the

nonimpulsive waveform (Fig. 6b) was judged to be relatively soft and was similar to a high pitched "buzz." These observations are consistent with those of other researchers on both full- and model-scale rotors.

The time-averaged spectra for this test point are shown in Fig. 7. The spectral levels have been adjusted (assuming 1/r variation of the Sound Pressure Level) for a distance of 11.2 rotor diameters to match FAA test parameters. The frequencies have not been shifted to match full-scale frequencies.

Figures 8 and 9 show acoustic waveform and spectra from the FAA full-scale hover test. Note in particular the presence of tail-rotor harmonics which are clearly identifiable. These, of course, are absent from the model-scale data.

The full-scale waveform is quite similar to the nonimpulsive waveform observed during the model test. A waveform corresponding to the impulsive waveform observed in the model-scale data was not clearly discernible in the full-scale data, except in isolated instances. This is somewhat surprising, because for hover in ground effect, recirculation of the wake is to be expected, which in turn leads to the expectation of variability of the acoustic waveform. This was not found to be the case.

Comparison of 1/3-octave spectra illustrates the persistence of high frequencies for the model. During the model hover test, wind-induced microphone self-noise was not a factor. Therefore, the observed high-frequency acoustic levels cannot be attributed to turbulence-induced microphone self-noise or to vortex shedding from microphone stands or other hardware. Full-scale data show rapid roll-off above 8 kHz, which, assuming geometrical scaling, corresponds to 48 kHz on model-scale. Model-scale data at such high frequencies were not obtained. The unweighted overall noise level for the model (when adjusted to the same distance) is within 3 dB of the full-scale level.

The first few blade-passage harmonic levels of the full-scale rotor were well reproduced by the model; however, the harmonics observed in the model spectra persist to approximately 4 kHz, whereas those in the full-scale data persist to only 500 Hz (corresponding to 3 kHz model-scale). Blade-passage harmonics persist for the model proportionately (assuming they scale geometrically) to somewhat higher frequencies, before being submerged in broadband sound, than they do for the full-scale rotor.

The full-scale data show a fairly steep (30-dB) roll-off in the 100-to-500-Hz range. The proportionately equivalent frequency range (600 to 3000 Hz) in the model-scale data shows a more gradual (20-dB) roll-off.

The full-scale/model-scale comparison presented here pertains mostly to the thickness-noise mechanism because of the small directivity

angle with respect to the rotor plane. Therefore, no conclusive statements regarding scaling of broadband noise mechanisms (which tend to be important at larger directivity angles) can be made. It should be noted that the recorded model-scale acoustic signals contained quite high frequency components at the effective response limits of the measuring system. This indicates that future tests will require very high performance instrumentation systems.

4. FORWARD FLIGHT TEST

Test Description

The forward-flight test was performed in the NASA Ames 7- by 10-Foot Wind Tunnel. The same 2.1-m diam four-bladed rotor as that described in Sec. 2 was mounted on the RTR in the standard thrust-up/wake-down mode (Fig. 10). The rotor hub was on the test-section centerline (approximately 1.1 m above the tunnel floor). The test model was installed on the tunnel six-component scale system. Rotor performance data were obtained from the tunnel scale system and independently from the internal balance.

The tunnel test section has optional foam-treated wall and ceiling panels. The acoustic characteristics of the soft-wall configuration were described by Soderman (Ref. 9). During the present test, an additional 7.5-cm-thick acoustic foam treatment was added upstream of the test section and on the floor to create an improved acoustic environment. Thus, in total, a 4.6-m length of the test section upstream of the model was covered on all four surfaces. There was some additional wall and ceiling foam treatment downstream. The leading edges of the foam treatment were carefully tapered to minimize separation and avoid the generation of additional turbulence. This relatively simple acoustic treatment of a limited length of the test section proved to be very effective in reducing wall reflections as determined by a series of pistol-shot sound measurements similar to those already described.

An array of nine microphones was mounted in the forward lower quadrant of the model at distances of 1, 1.5, and 2 rotor diameters and at various azimuthal and elevation angles (Fig. 11). Several of these microphones duplicated the relative positions of corresponding microphones used during a full-scale S-76 rotor wind-tunnel test (Ref. 6). Physical limitations prevented the positioning of the microphones at large angles below the rotor plane. Therefore, while thickness noise was readily detectable, loading noise was not. The lower microphones were marginally located to detect blade-vortex interaction noise. The microphone stands were fabricated from 2.2-cm-thick streamlined tubing. Laminar shedding tones were avoided by applying tape to the leading edges of the stands to act as boundary-layer trips.

Acoustic signals were measured with 0.635-cm, free-field response-type microphones, mounted parallel with the flow. Standard nose cones were fitted over the cartridges. Microphone outputs were

recorded on a 14-track FM instrumentation tape recorder set up to IRIG Wideband I standards at 60 in./sec (152.4 cm/sec). The system frequency response was good to approximately 35 kHz. 1/rev, 1024/rev, and time-code signals were also recorded. Test conditions, and amplifier information were annotated on the voice track.

System frequency-response checks similar to those described in Sec. 2 were made. Additional tests with a small jet source were made to check high-frequency response. Piston-phone calibrations were performed before each day's testing.

Forward Flight Performance Results

The primary variables during the wind-tunnel test were tip Mach number, tunnel Mach number, rotor-shaft angle, and rotor lift coefficient (Table 3). These values were chosen to duplicate some of the test conditions of the full-scale wind-tunnel test performed in the 40- by 80-Foot Wind Tunnel (Ref. 5).

Figures 12 and 13 summarize the model-rotor performance data in forward flight. Data from the full-scale test in the 40- by 80-Foot Wind Tunnel are also shown. A rotor system that had the same airfoil (Sikorsky SC1095 used on the S-76) as the model rotor was used in the full-scale test. Data on four sets of tips were acquired during the full-scale test; the tips in one of those sets had rectangular profiles (same as the model tips), and is the one on which the comparison in the figures is based.

Figure 12 is a plot of lift-to-drag ratio for a flight speed of 150 knots, a common cruise speed. The maximum L/D is approximately 15% higher for the model rotor. The maximum L/D was obtained at typical cruise C_L/σ of 0.07 for the full-scale rotor but at lower values for the model. This shifting of the L/D curve (at fixed μ) was typical of all of the data.

Figure 13 is a comparison of lift-to-drag ratio as a function of advance ratio for a thrust condition, $C_L/\sigma = 0.085$, near the crossover point of Fig. 12. Here again there is a significant difference (approximately 10%) in the maximum L/D between full-scale and model-scale. However, now the maxima occur at the same speed (120 knots). This was observed to be true at all thrust levels.

That the model-scale rotor performance is better than full-scale performance is unexpected. The reasons for this are being investigated. The possible reasons for the better performance of the model-scale rotor include the following: (1) incorrect scaling of control system stiffness, thereby influencing dynamic pitch in forward flight; (2) aerodynamic surface discontinuities at the junction of the full-scale rectangular tip and the blade; and (3) differences in the aerodynamic interferences between the respective rotor systems and their test stands.

Forward Flight Acoustic Results

Accustic data obtained during the wind-tunnel test are summarized in Figs. 14-16. Figure 14 is an illustration of the general trends of the overall acoustic levels as a function of tip speed, tunnel speed, thrust, and shaft angle. $M_{1,90}$ is the advancing-tip Mach number. The data are for microphone No. 3 which was 10° below the rotor plane at a distance of 1.5 rotor diameters. At this location, the dominant mechanism is expected to be thickness noise, mostly low-frequency harmonic in spectral content.

The strong dependence of acoustic levels on advancing-tip Mach number is clear (Fig. 14a), whereas the dependence on advance ratio is somewhat weaker, as indicated by the close clustering of data points about the faired line (Fig. 14b). Note the sharp rise in acoustic levels above an advancing-tip Mach number of 0.87, The dependence on rotor lift and shaft angle are also weak (Figs. 14c and 14d), as is to be expected for directivities near the rotor plane, where loading noise is less dominant than thickness noise.

Figure 15 shows 1/3-octave and narrow-band spectra corresponding to the points labeled A, B, and C on Fig. 14a. Background noise levels are indicated on the 1/3-octave spectra. Clearly, high-frequency broadband noise was not adequately measured, because of high background noise levels. At high rotor tip speeds (cases A and C), the signal-to-noise ratio of low- and mid-frequency harmonic components was quite adequate even at high tunnel speeds. For low tip speed (case B), only the first few harmonics of blade-passage frequency are discernible above the background level.

The relatively high peak in the 40-Hz 1/3-octave band at high tunnel speed (cases A and B), and its absence at the low tunnel speed (case C), indicates the presence of either tunnel-drive fan harmonics or a low-frequency flow unsteadiness in the test section at high speeds, especially since the peak occurs at a frequency below blade-passage frequency (125 Hz). This flow pulsation could affect rotor aerodynamics, in turn affecting rotor acoustics. This effect was not studied during this test.

Comparison of cases A and C shows an increase in the level of blade-passage harmonics at the higher advance ratio. Interestingly, the level of the fundamental itself remains unchanged. Since the advancing-tip Mach number for case A is approximately 0.9, local shock waves undoubtedly are present, which, coupled with flow unsteadiness, may well be the origin of the rich mid-frequency spectral content.

For case A, the spectral levels at higher frequencies are generally higher. This is attributed to the increase in background noise at the higher tunnel speed rather than to high-frequency broadband mechanisms such as trailing-edge noise, particularly since the directivity angle is small. The origin of the peak at 3.5 kHz is not known.

These trends were generally found to hold also for microphones 4 and 6, which are, respectively, 5° below and 16° lateral to microphone 3. There were only minor differences in spectral content and the overall sound pressure levels were within 2 dB.

Figure 16 is a comparison of the model-scale acoustics data and the full-scale data obtained in the 40- by 80-Foot Wind Tunnel (Ref. 6). At the time of the test, the tunnel test section had no acoustic treatment. Therefore, the comparison is strictly valid only for high-level harmonic components radiating within a small directivity angle near the rotor plane. The comparison is made on the basis of 1/3-octave spectra. The full-scale data were shifted over in frequency so that the blade-passage frequency band coincided with the model-scale data. No adjustments in level were made, because it was assumed that the full-scale data were mostly harmonic and not broadband in nature at the lower frequencies of interest, as was the case for the model-scale data.

Generally, the model-scale data did not predict full-scale levels well. The full-scale data fall approximately 5-10 dB higher than the model-scale data. This holds true for both tip speeds. Recalling that the full-scale data were obtained in an untreated tunnel, the differences are expected and may, to some extent, be attributable to reverberation effects. Full-scale forward-flight data in the treated 40- by 80-Foot Wind Tunnel will be obtained in the future so that further comparisons can be made.

5. CONCLUSIONS

The performance and acoustics of a small-scale rotor were compared with those of a full-scale rotor in both hover and forward flight.

The hover performance and acoustic results for the model-scale and full-scale rotors compared quite well. The expected Reynolds-number influence on profile power was evident. Acoustic low-frequency harmonic levels were found to scale geometrically. At full-scale mid-frequencies, the spectral levels rolled-off much more rapidly than model-scale data at equivalent frequencies. Model-scale data at equivalent full-scale high frequencies were not available. However, there are strong indications of significant model-scale spectral content at quite high frequencies.

In forward flight, both the performance and acoustics of the small-scale rotor compared poorly with the full-scale data. Significant Reynolds-number effects were found in the lift-to-drag comparison. The acoustic spectra of both the model- and full-scale rotors exhibit similar trends; however, there was an overall difference in levels of 5-10 dB.

REFERENCES

1. F. H. Schmitz, D. A. Boxwell, S. Lewy, and C. Dahan, A Note on the General Scaling of Helicopter Blade-Vortex Interaction Noise. Paper presented at the 38th Annual National Forum of the American Helicopter Society, Anaheim, Calif., May 1982.

2. D. A. Boxwell, F. H. Schmitz, W. R. Splettstoesser, and K. J. Schultz, Helicopter Model Rotor Blade Vortex Interaction Impulsive Noise: Scalability and Parametric Variations. Paper presented at the 10th European Rotorcraft Forum, the Hague, Netherlands, Aug. 1984.

3. F. H. Schmitz, D. A. Boxwell, W. R. Splettstoesser, and K. J. Schultz, Model-Rotor High Speed Impulsive Noise: Full-Scale Comparisons and Parametric Variations. Vertica, vol. 8, no. 4, 1984, pp. 395-422.

4. K. P. Leighton, S. D. Roth, and F. Kohlhepp, 1/20-th Scale Helicopter Rotor Acoustics Characteristics in an Anechoic Wind Tunnel. NASA CR-177355, 1985.

5. W. Johnson, Performance and Loads Data from a Wind Tunnel Test of a Full-Scale Rotor with Four Blade Tip Planforms. NASA TM-81229, 1980.

6. M. Mosher, Acoustic Measurements of a Full Scale Rotor with Four Tip Shapes. NASA TM-85878, 1984.

7. D. Jepson, R. Moffitt, K. Hilzinger, and J. Bissel, Analysis and Correlation of Test Data from an Advanced Technology Rotor System. NASA CR-3714, 1983.

8. J. S. Newman, E. J. Rickley, T. L. Bland, nd K. R. Beattie, Noise Measurement Flight Test: Data Analysis, Sikorsky S-76A Helicopter. Report FAA-EE-84-6, Federal Aviation Administration, 1984.

9. P. T. Soderman, Instrumentation and Techniques for Acoustic Research in Wind Tunnels. Paper presented at 6th International Congress on Instrumentation in Aerospace Simulation Facilities, Ottawa, Canada, 1975.

Table 1. Model-rotor characteristics

Radius, R	1.0668 m
Chord, C	6.2941 cm
Airfoil	SC1095/SC1095R8
Number of blades	4
Twist	-10° linear
Solidity, σ	0.075121

Table 2. Test parameters for scaling comparison of hover noise

	Model scale	Full scale (FAA)
Airfoil	SC1095/SC1095R8	SC1095/SC1095R8
Blade tip	Rectangular	Swept tapered
M_{tip}	0.55	0.59
C_T/σ	0.09	0.09 (estimated)
Angle of microphone from rotor plane	10°	2°
Microphone distance	11.2 rotor diam (adjusted)	11.2 rotor diam

Table 3. Forward-flight test parameters

Rotor tip Mach number, M_{tip}	0.55, 0.6, 0.65
Tunnel Mach number, M_{tun}	0.12, 0.18, 0.225, 0.25
Rotor shaft angle, α_s	-10°, -5°, -2.5°, 0°, +6°
Rotor lift coefficient, C_L/σ	0.03 - 0.12

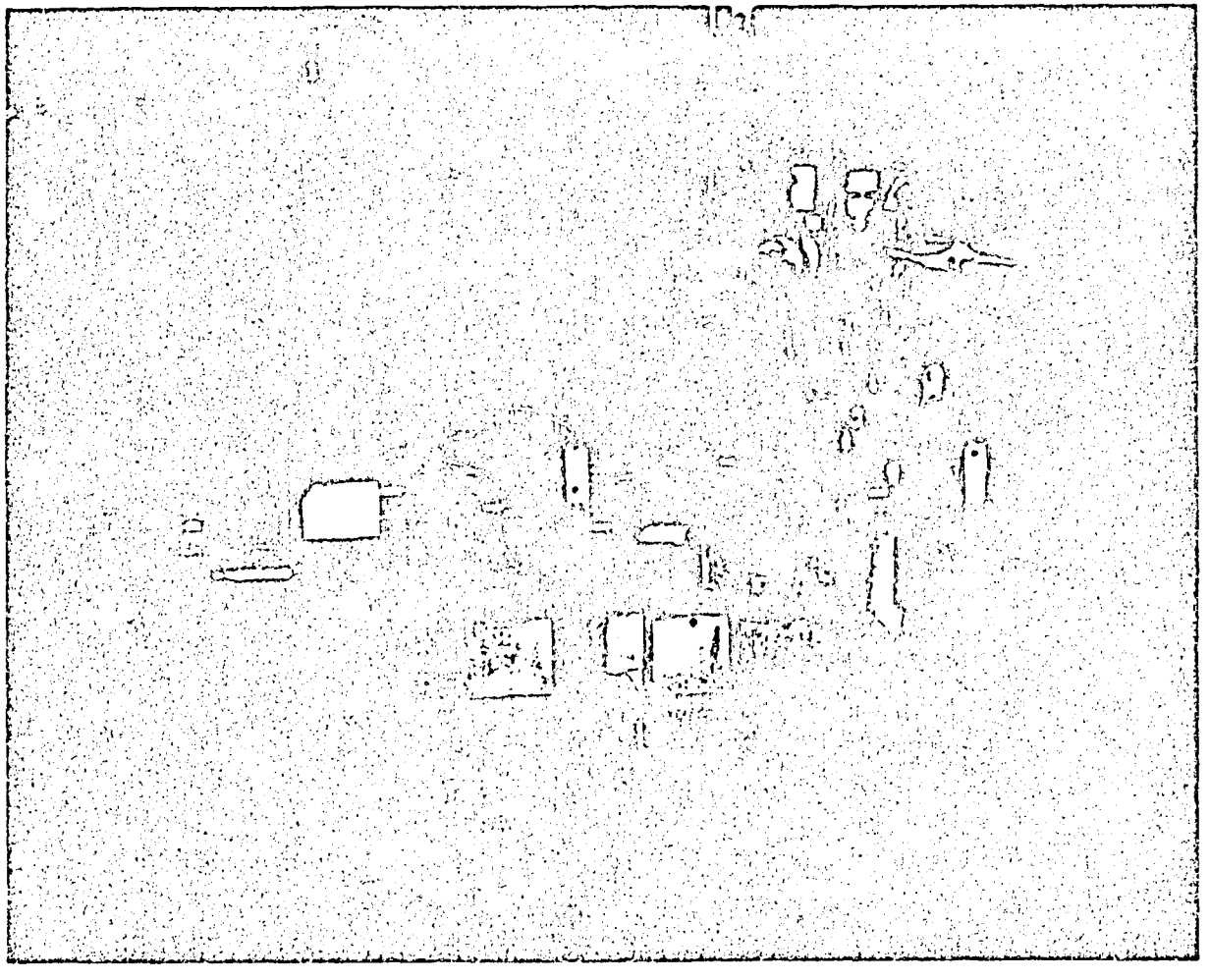

Fig. 1. NASA Ames Rotor Test Rig with club blades.

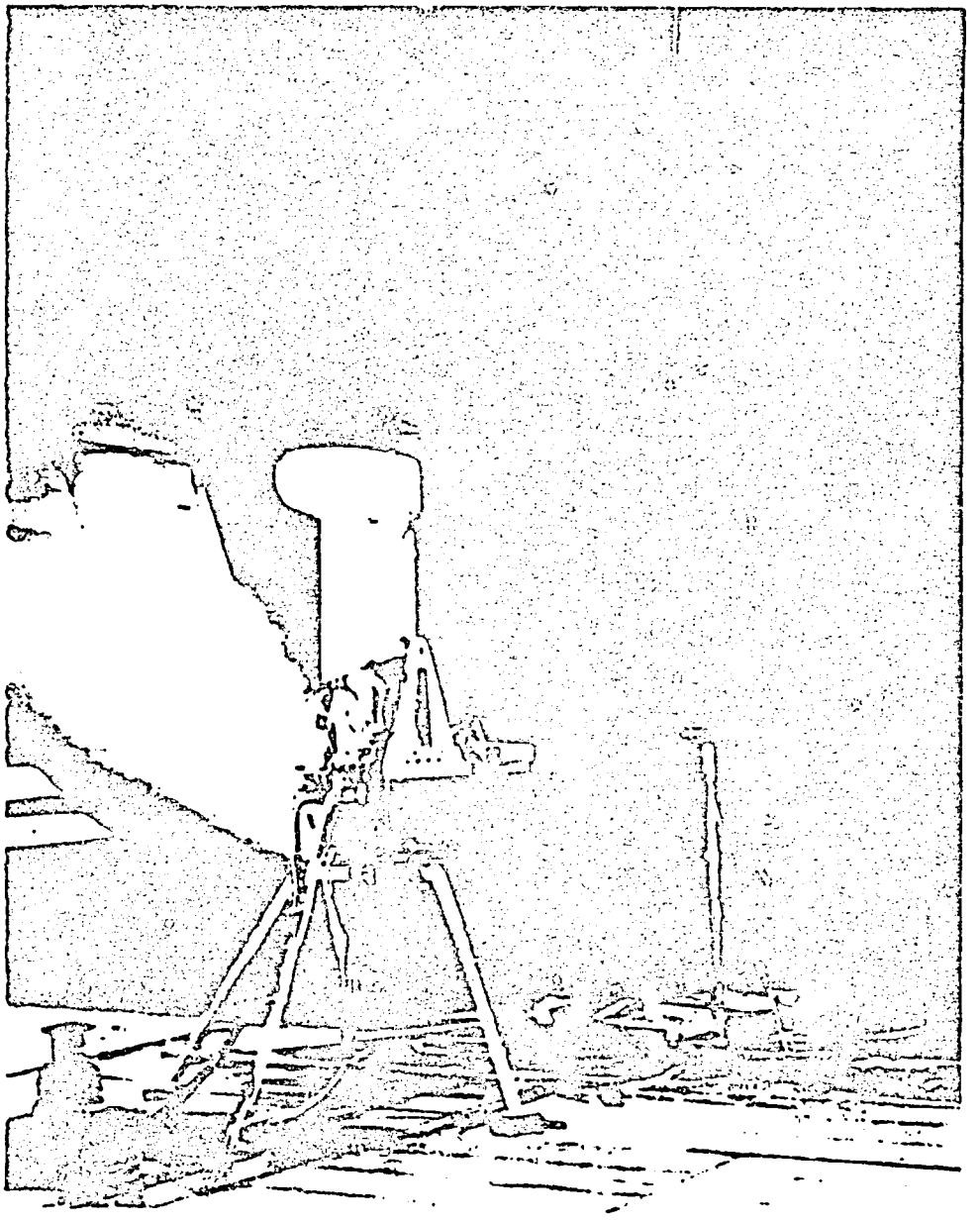

Fig. 2. Rotor Test Rig and microphone array mounted in NASA Ames 40- by 80-Foot Wind Tunnel test section for hover test.

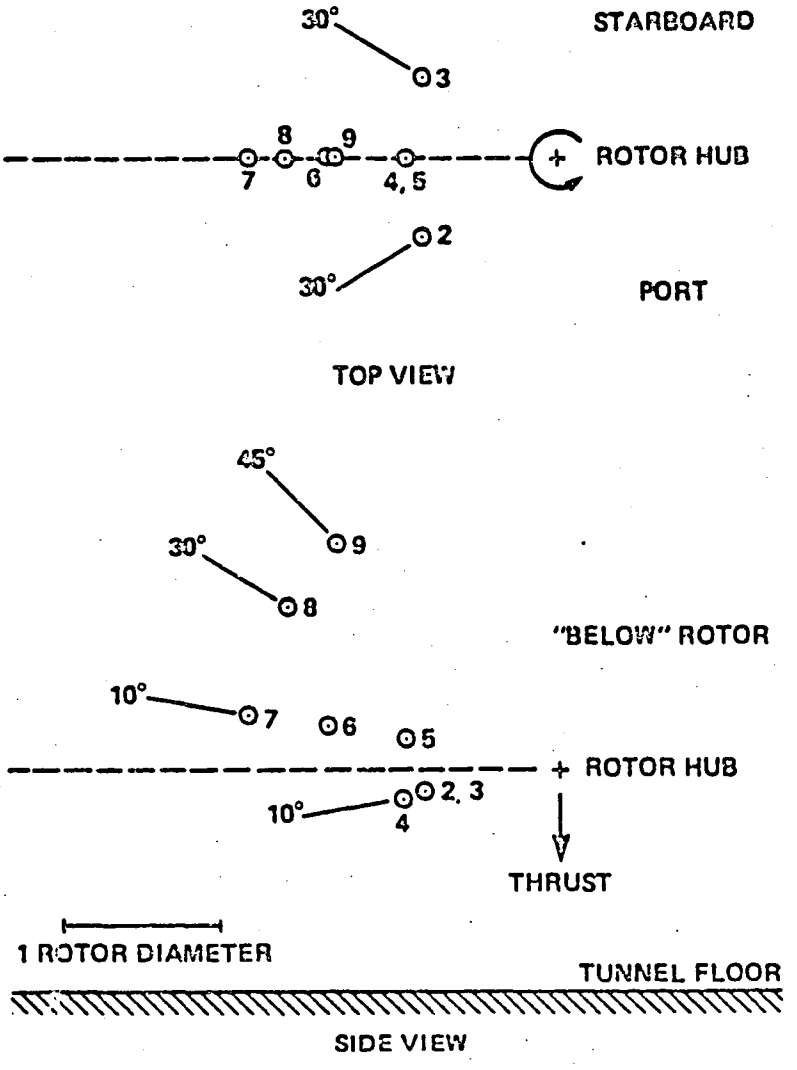

Fig. 3. Microphone array for hover test.

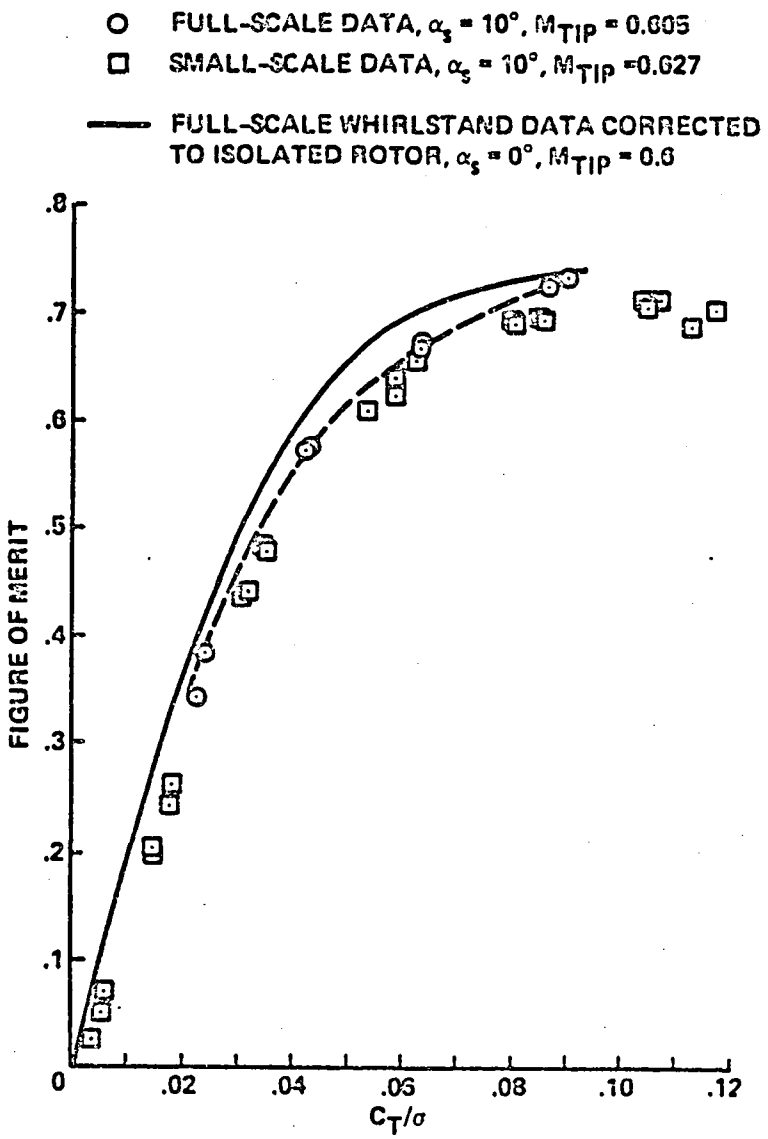

Fig. 4. Hover performance and comparison with full-scale data: Figure of Merit.

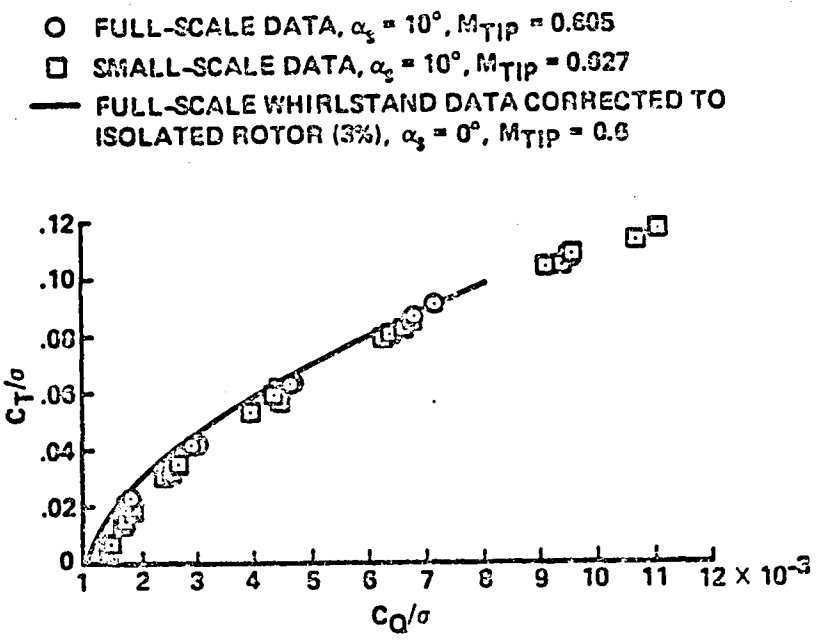

Fig. 5. Hover performance and comparison with full-scale data: Thrust vs. Torque.

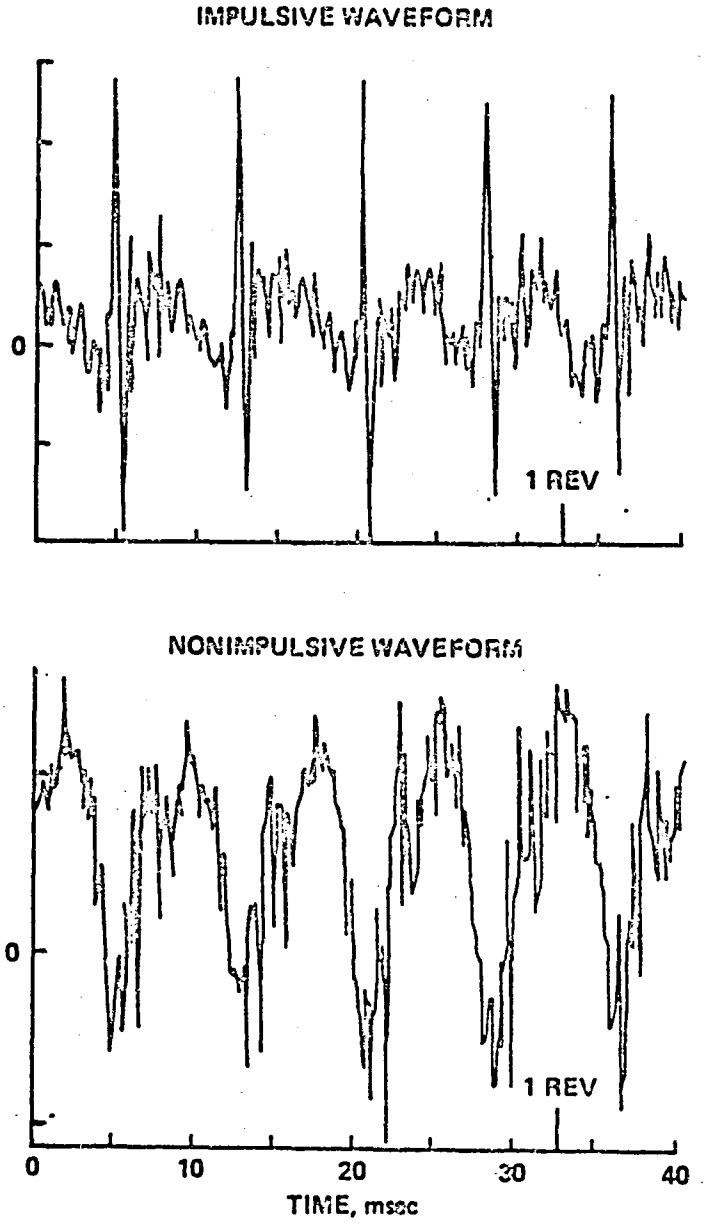

Fig. 6. Small-scale model rotor hover noise data.

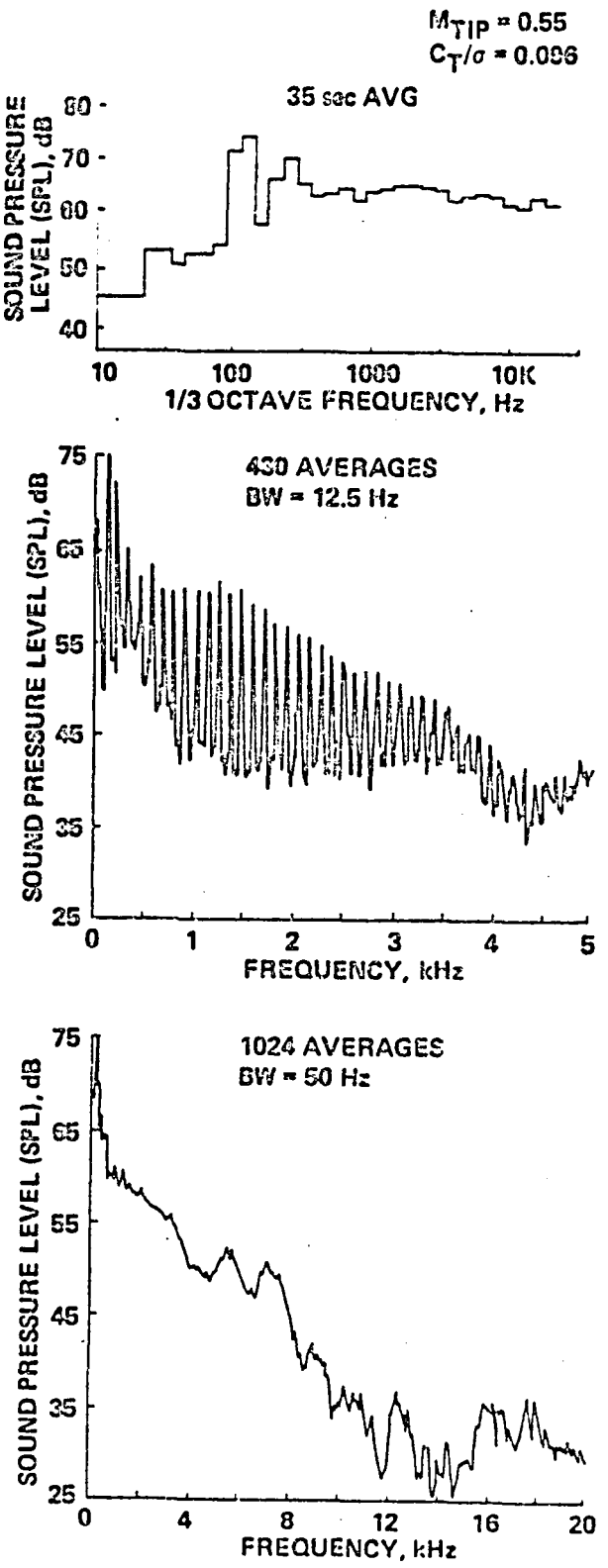

Fig. 7. Small-scale model rotor hover acoustic spectra. Levels adjusted for distance of 11.2 rotor diameters.

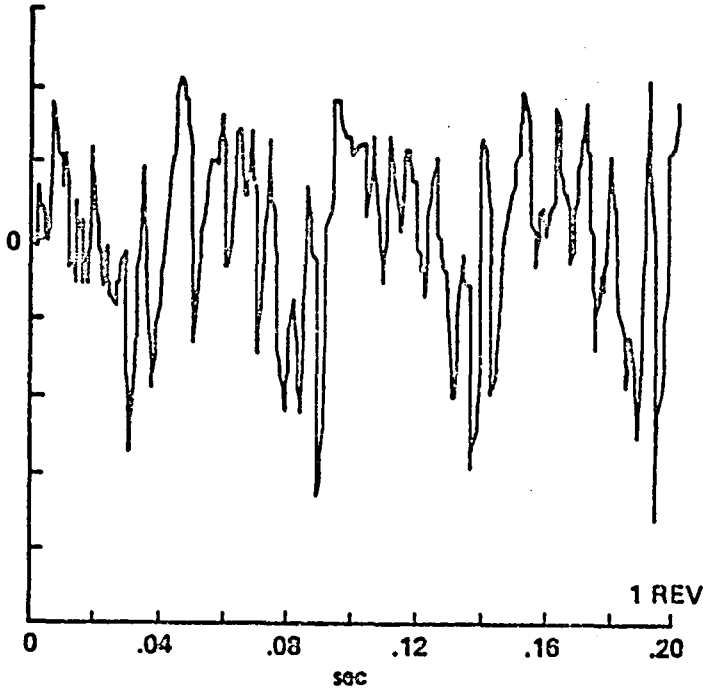

Fig. 8. Full-scale aircraft hover acoustic waveform.

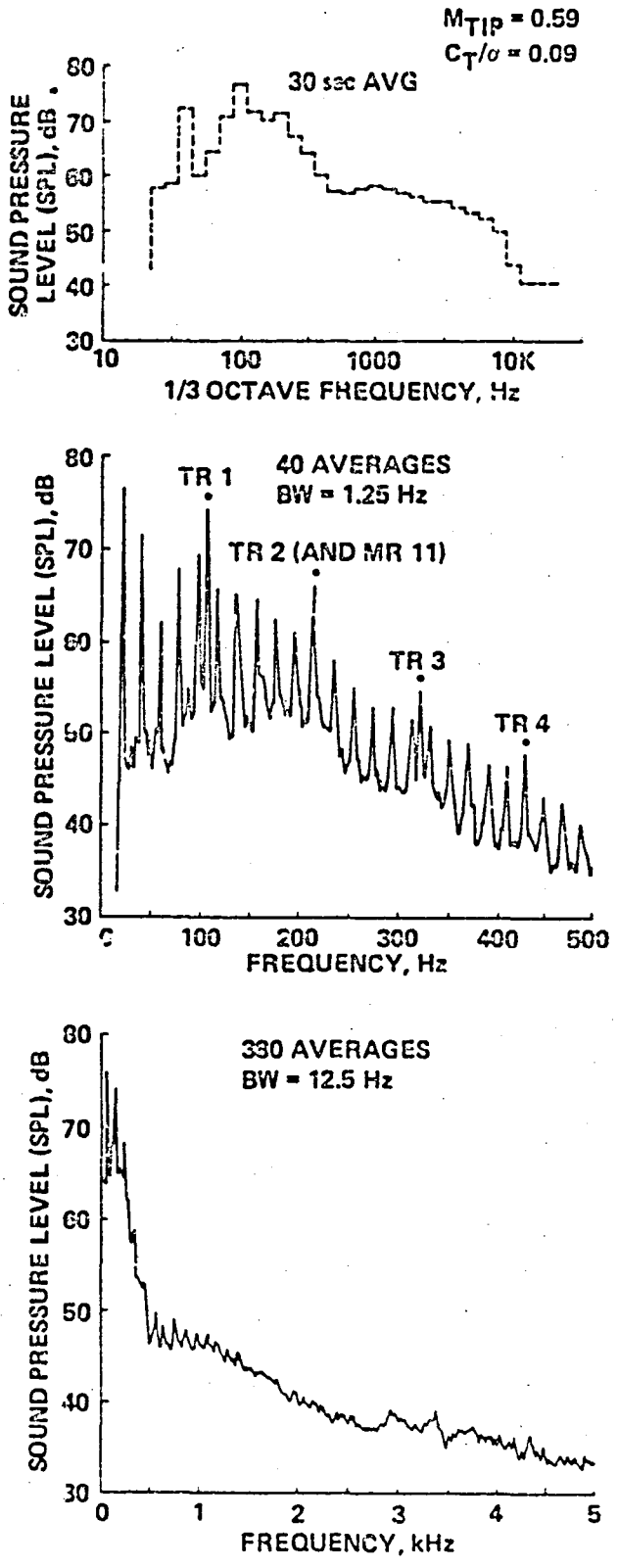

Fig. 9. Full-scale aircraft hover acoustic spectra.

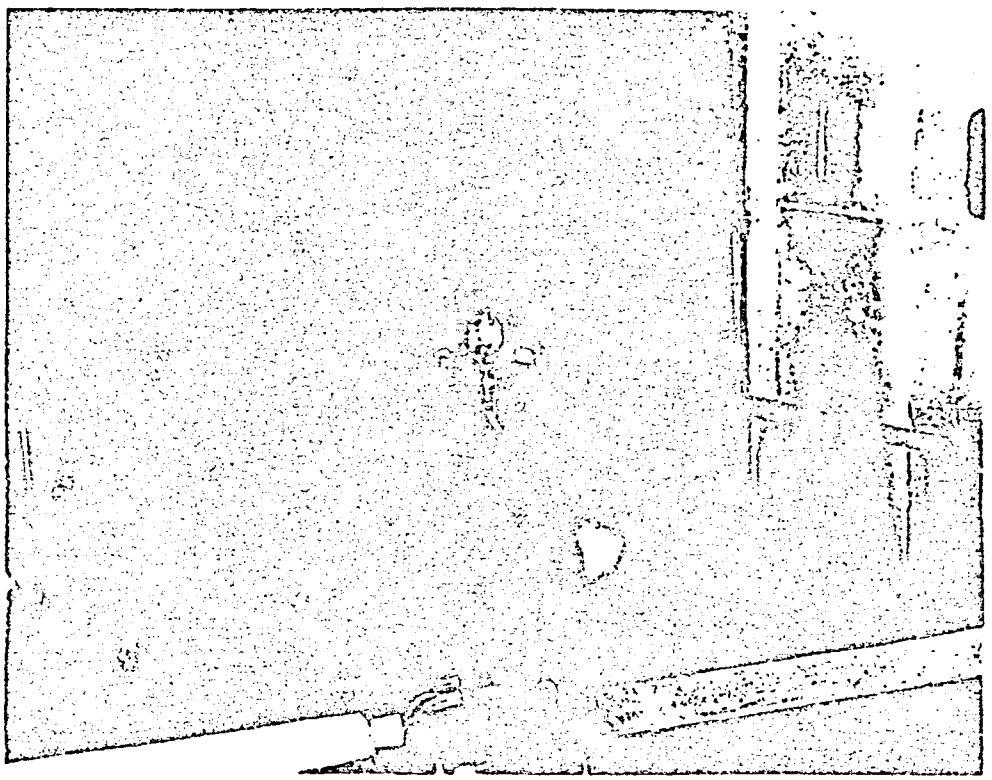

Fig. 10. Rotor Test Rig and microphone array mounted in NASA Ames 7- by 10-Foct Wind Tunnel.

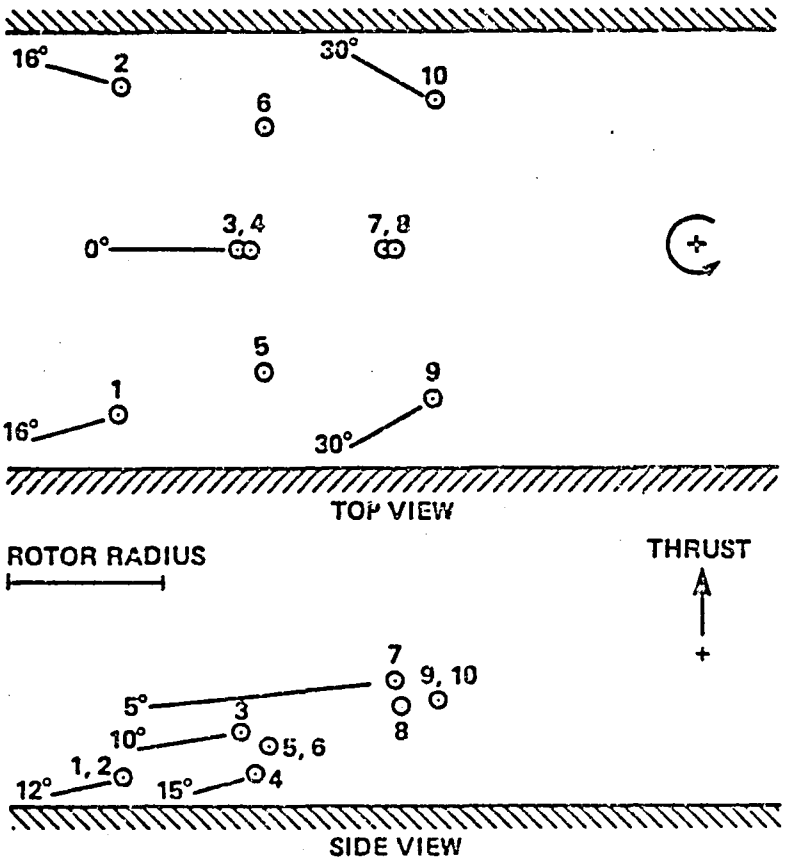

Fig. 11. Microphone array for forward flight test.

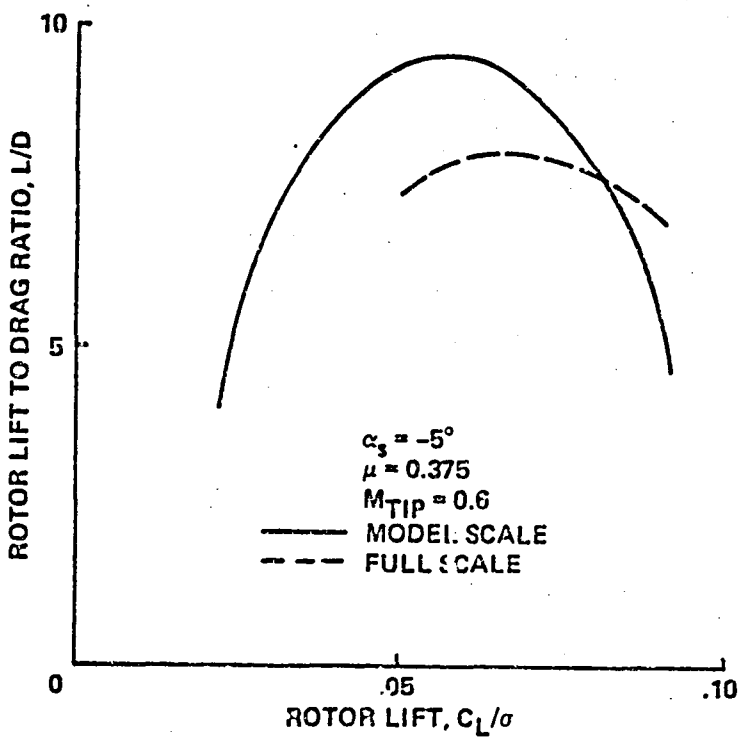

Fig. 12. Forward flight performance: L/D vs. C_L/σ.

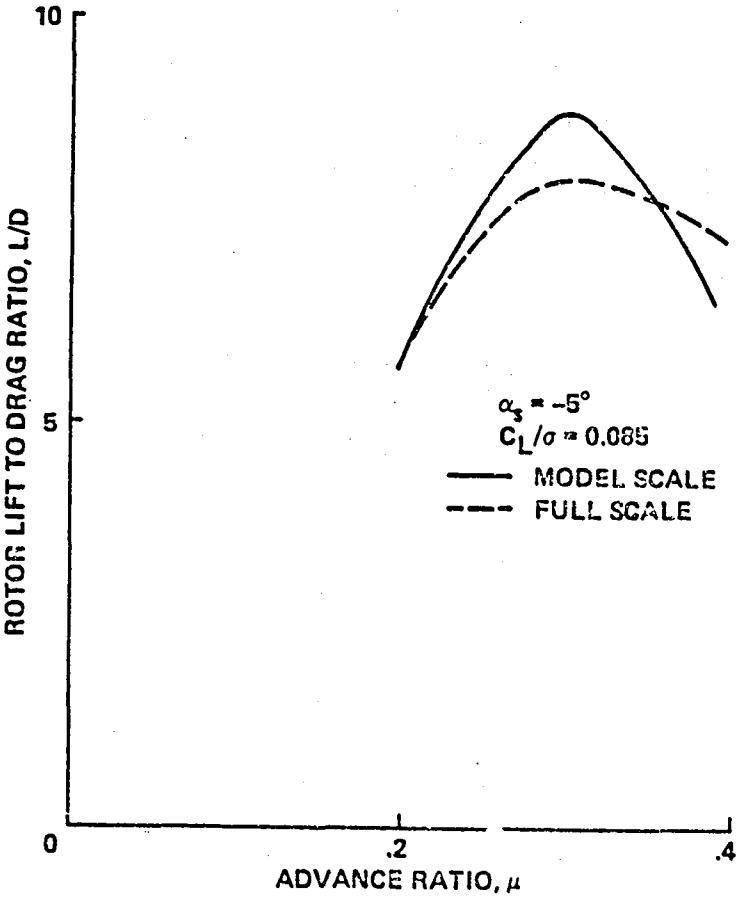

Fig. 13. Forward flight performance: L/D vs. μ.

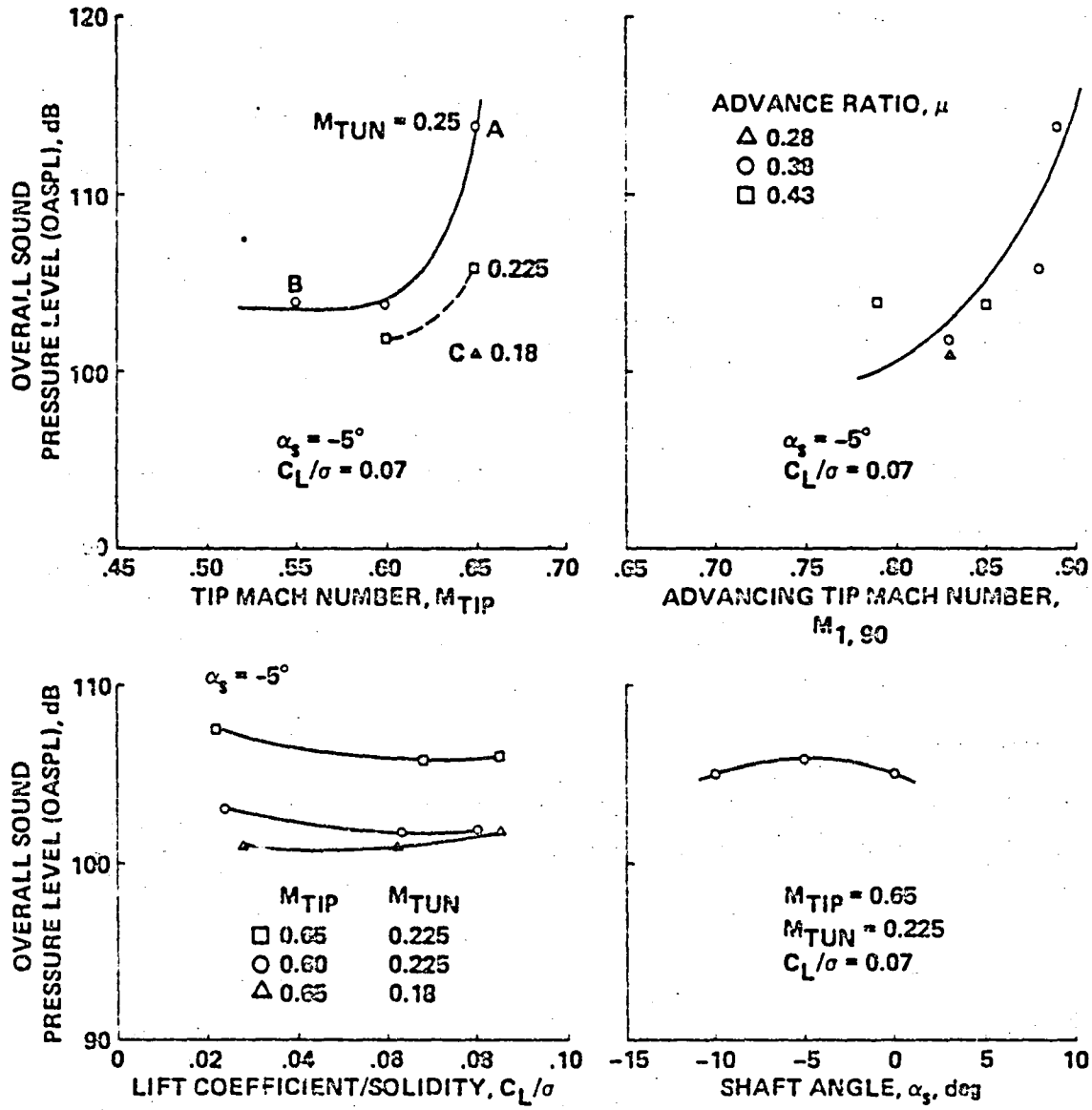

Fig. 14. Small-scale model rotor forward flight acoustic data: OASPL as a function of test parameters. (Microphone no. 3; ψ = 180°, θ = 10°, r/D = 1.5.)

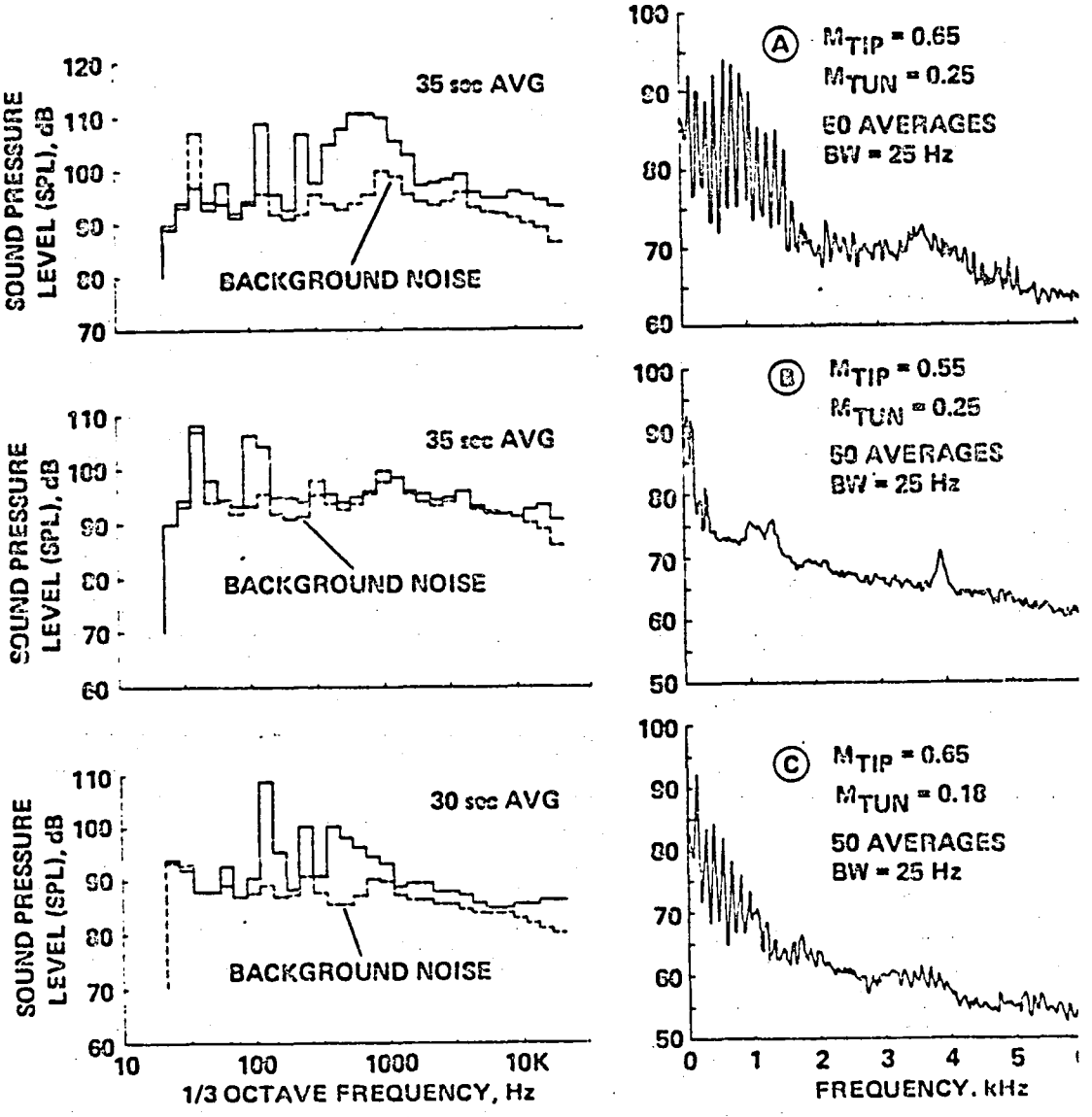

Fig. 15. Small-scale model rotor forward flight acoustic data: spectra. (Microphone no. 3; ψ = 180°, θ = 10°, r/D = 1.5.)

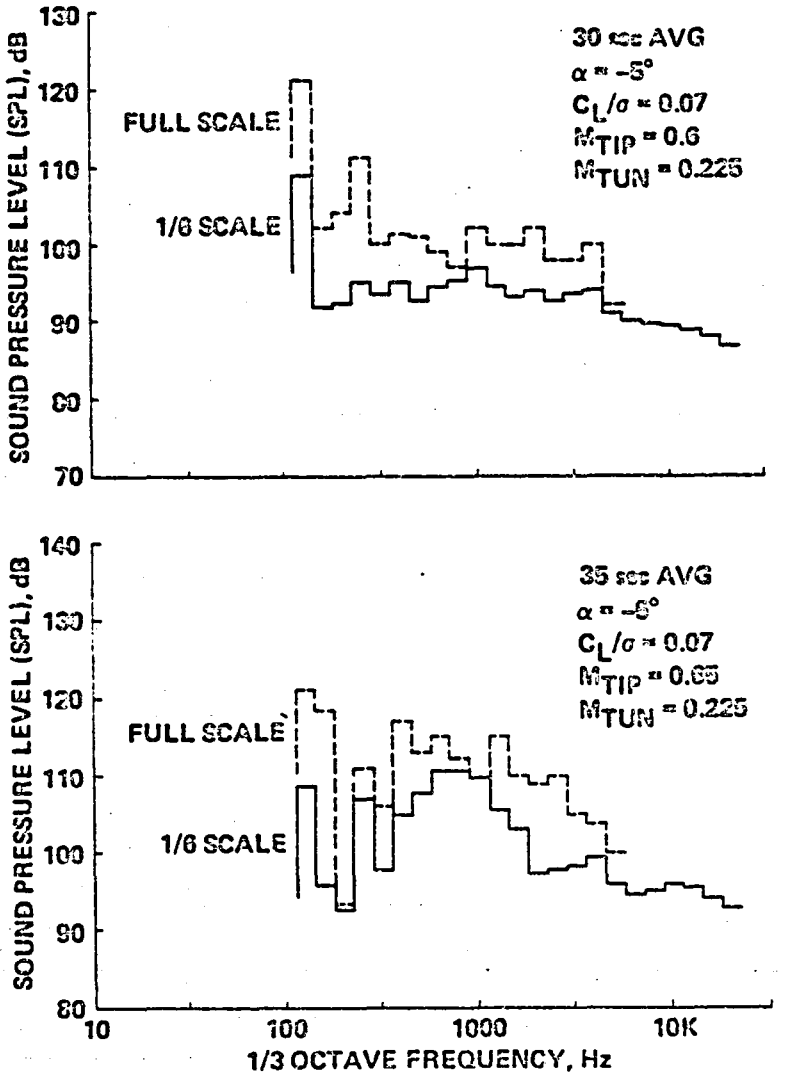

Fig. 16. Forward flight acoustic data: comparison with full-scale. (ψ = 180°, θ = 10°, r/D = 1.5.)

END

FILMED

12-85

DTIC